doi: 10.18323/2782-4039-2023-2-64-2

The formation of highly dispersed zinc oxide powder during combustion of zinc nitrate with glycine mixture and its application for photocatalytic phenol decomposition

Aleksandr P. Amosov*[1,3], Doctor of Sciences (Physics and Mathematics), Professor,
Head of Chair "Metals Science, Powder Metallurgy, Nanomaterials"
Vladislav A. Novikov[1,4], PhD (Engineering),
assistant professor of Chair "Metals Science, Powder Metallurgy, Nanomaterials"
Egor M. Kachkin[1,5], student
Nikita A. Kryukov[1,6], student
Aleksandr A. Titov[1,7], student
Ilya M. Sosnin[2,8], junior researcher at the Research Institute of Advanced Technologies
[1]*Samara State Technical University, Samara (Russia)*
[2]*Togliatti State University, Togliatti (Russia)*

***E-mail: mvm@samgtu.ru**
egundor@yandex.ru

[3]ORCID: https://orcid.org/0000-0003-1994-5672
[4]ORCID: https://orcid.org/0000-0002-8052-305X
[5]ORCID: https://orcid.org/0000-0002-4745-2237
[6]ORCID: https://orcid.org/0000-0001-6900-4278
[7]ORCID: https://orcid.org/0000-0001-8707-6523
[8]ORCID: https://orcid.org/0000-0002-5302-3260

Received 13.07.2022 *Accepted 02.05.2023*

Abstract: The paper presents the results of a detailed study of the process and products of combustion during self-propagating high-temperature synthesis (SHS) of ZnO zinc oxide powder from mixtures of such common reagents as oxidizer zinc nitrate and reducing agent (fuel) glycine, as well as the application of synthesized highly dispersed submicron and nanosized ZnO powder for the phenol photocatalytic decomposition under the action of ultraviolet irradiation. An aqueous solution of a mixture of reagents (the SHS-S process or Solution Combustion Synthesis – SCS) and the gel from a mixture of initial dry reagents formed when they were moistened due to hygroscopicity (the SHS-G process or Gel Combustion Synthesis – GCS) were combusted. The authors studied the phase and chemical compositions, the structure of the combustion product, and the effect of calcination in an oxidizing air medium and grinding in drum ball and planetary-centrifugal mills, as well as in mortar, on them and their photocatalythic activity. The study showed that calcination considerably increases the photocatalytic activity of combustion products due to a significant decrease in carbon impurity in the unburned fuel remains, and grinding in mills reduces the photocatalytic activity due to iron contamination and coarsening of ZnO particle agglomerates. The difference between the photocatalytic activity of the SHS-G and SHS-S products in the phenol decomposition is evident only at the initial stage of ultraviolet irradiation, after which this difference disappears. The authors discuss the direction of further research to increase significantly the photocatalytic activity of zinc oxide synthesized during combustion to use it effectively for the phenol decomposition under the action of visible light.

Keywords: highly dispersed zinc oxide powder; zinc oxide; zinc nitrate and glycine mixture; photocatalytic phenol decomposition; combustion; self-propagating high-temperature synthesis; ZnO.

Acknowledgments: The work was carried out under the financial support of the Russian Science Foundation within the project No. 22-29-00287.

For citation: Amosov A.P., Novikov V.A., Kachkin E.M., Kryukov N.A., Titov A.A., Sosnin I.M. The formation of highly dispersed zinc oxide powder during combustion of zinc nitrate with glycine mixture and its application for photocatalytic phenol decomposition. *Frontier Materials & Technologies*, 2023, no. 2. DOI: 10.18323/2782-4039-2023-2-64-2.

INTRODUCTION

Recently, the problem of wastewater pollution and purification from such a highly toxic organic compound as phenol C_6H_5OH and its derivatives has become particularly acute [1]. Among various methods of water purification from this pollutant, the most effective and environmentally friendly is the use of photocatalysts – materials decomposing organic pollutants under the action of electromagnetic radiation (visible or ultraviolet light), without the formation of residual toxic compounds. Highly dispersed nanosized and submicron powder of zinc oxide ZnO is considered one of the most promising, in application, as a heterogeneous photocatalytic material for the degradation of organic pollutants [2–4].

There are quite a few methods for synthesis of ZnO-based nanomaterials, which can be divided into two groups: solution and gas-phase [3; 4]. Gas-phase methods are complex, implemented on expensive equipment, energy-intensive, and inefficient. Simpler and less energy intensive solution methods make it possible to effectively control

the composition, morphology, and size of synthesized ZnO nanopowders using such factors as the type of solvent, composition of re-agents, and synthesis conditions. However, both types of methods are characterized by low productivity, which prevents the organization on their basis of industrial production of nanostructured ZnO photocatalysts for wastewater purification.

The method of solution self-propagating high-temperature synthesis (SHS) of oxides in the combustion mode differs noticeably from the methods listed above, in its simplicity, energy saving, and high productivity, which makes it attractive for creating technologies, for the industrial production of various low-budget oxide nanomaterials for manifold uses [5–7]. The method of solution SHS (SHS-S) is based on the combustion of a mixture of dissolved, most often in water, re-agents of exothermic redox reactions or on the combustion of a gel from a mixture of dry re-agents (SHS-G), therefore it is also called synthesis during solution combustion (Solution Combustion Synthesis – SCS) or synthesis during gel combustion (Gel Combustion Synthesis – GCS).

A gel from a mixture of re-agents is formed, both in the SHS-S process from a mixture of aqueous solutions of re-agents after solvent evaporation, and in the SHS-G process when mixing dry re-agents, which is accompanied by their spontaneous moistening from the ambient air due to hygroscopicity. Thus, in both cases, the oxide nanopowder synthesis occurs during gel combustion. There are studies on the possibility of obtaining ZnO during the combustion of gels, but they do not describe the process and combustion products in sufficient detail, which makes it difficult to choose them for reasonable practical application [8–10].

This work [11] presents the results of a detailed study of the SHS-S process of zinc oxide ZnO nanopowder from a solution of a mixture of such common re-agents as the oxidizing agent zinc nitrate $Zn(NO_3)_2$ and the reducing agent (fuel) glycine $C_2H_5NO_2$, as well as the use of synthesized ZnO for the phenol photocatalytic decomposition. Let us present the results of this study in more detail, since this work is a continuation of [11].

The results of these experimental studies [11] demonstrate that when heating a vessel with an aqueous solution of zinc nitrate and glycine re-agents at h=6.5 mm and T_S=460 °C, after water evaporation and gel formation (on average for 8 min at $0.5 \le \varphi \le 1.5$), the reaction proceeds in the mode of rapid (≤3 s), overall combustion with a yellow flame and a sudden, almost complete release of the reaction mixture and milky reaction products in the form of thick white smoke (pure ZnO is white) from the vessel. This is clearly illustrated in Fig. 1 by the close to zero values of the product mass conservation coefficient $K_M(\varphi)$ in the range of $0.5 \le \varphi \le 1.5$ obtained as a result of three experiments for each value of the criterion φ.

Fig. 1 shows that the combustion characteristic values obtained in three experiments for the same criterion φ value can differ significantly from each other, that is, they have a large spread. With a reduced fuel content φ=0.25, the reaction proceeds in a flameless mode with a rapid release of red smoke for 2–5 s and a partial emission of a light-green product. When φ>1.5, the combustion and product appearance change. When increasing φ, a transition to synthesis in the mode of progressively slower smoldering (up to 3 min in average) occurs, the color of the loose product changes from grey with an admixture of white to black, with an admixture of white. At φ=2.5 and more, the color becomes completely black, and the product mass conservation coefficient K_M at φ>2 becomes even greater than one.

According to [11], at $0.5 \le \varphi \le 1.5$, the SHS-S reaction proceeds in the most intense explosive mode, due to the closeness to the optimal ratio of fuel and oxidizer at φ=1

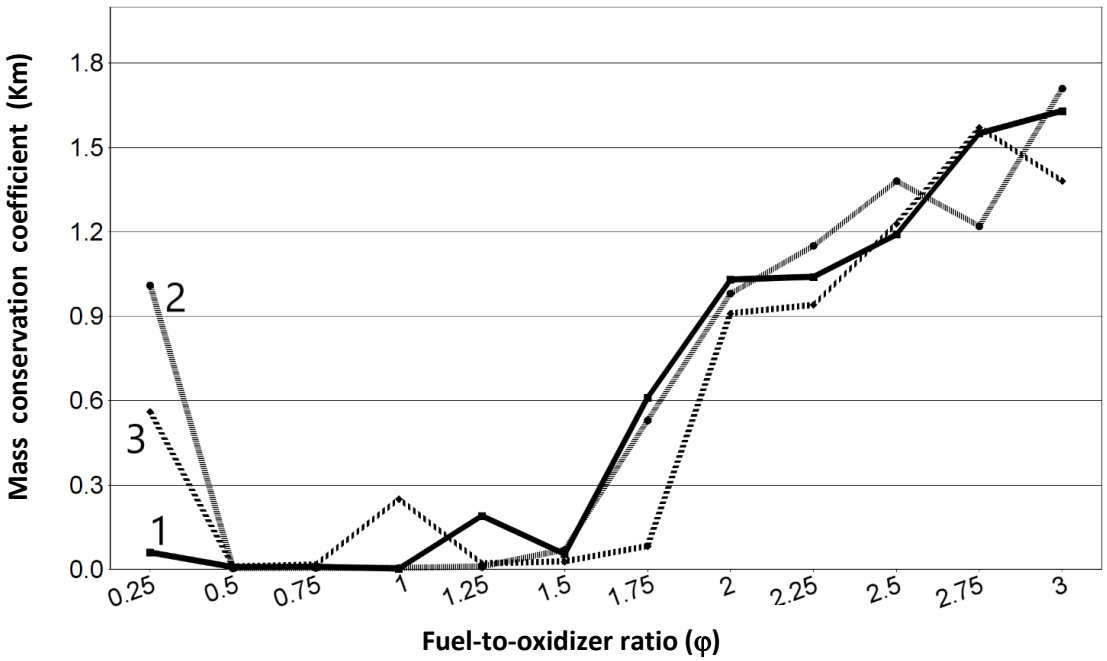

Fig. 1. *The dependence of the product mass conservation coefficient K_m on the value of the criterion φ at the combustion of the solution of re-agents [11, p. 932]. The numbers on the lines indicate the numbers of experiments*

with a sudden, almost complete release of the product from the reaction vessel. At φ<0.5 and at φ>1.5, the initial mixture of re-agents in the solution contains an excess of oxidizer or fuel, respectively, and the reaction of solution SHS of zinc oxide proceeds in a quieter mode without a sudden release of the product from the vessel, especially at φ≥2.

In this range of φ values, changes in the product colour and mass are explained by the fact that at φ>1.5, the mixture of re-agents becomes fuel-rich, it lacks internal oxygen in the mixture of re-agents and external oxygen from the ambient air for complete oxidizing of carbon in the fuel, and its removal from the combustion product in the form of CO_2. The combustion product, along with pure white ZnO, contains an increasing amount of black free carbon and unburned fuel residues; at φ>2, its color is completely black, and the mass exceeds the theoretical yield of ZnO, and therefore the K_M coefficient becomes greater than one [11]. In this case, for the reaction to proceed throughout the entire volume of the mixture of re-agents, it is necessary to stir constantly this mixture during smoldering. Following these results, one can conclude that the value φ=2 is the most suitable for practical use; with this value, there is no explosive combustion with the release of the product from the vessel, observed at lower φ, and intense smoldering in about 8 s leads to the formation of an easily destructible powder with its retention in a vessel without the need for constant stirring to complete the synthesis reaction, which is required when φ>2.

Fig. 2 shows the combustion product microstructure for φ=2 in the form of a frozen foamy mass with a large number of pores of various diameters and agglomerates of small nanosized and submicron ZnO particles [11].

In Fig. 2, an amorphous component is represented by foam due to the solidification of the gel-like residue in the combustion product. Such a residue is present as a consequence of the formation of free carbon in amorphous form, and carbon bound with oxygen and hydrogen in unburned fuel residues, as shown in [12; 13].

The carbon content in the SHS-S product at φ=2 reaches almost 10 % in average [11]. When performing oxidative annealing (calcination) of the combustion product for 1 h at 650 °C in a muffle furnace with an air atmosphere, the carbon content decreases to an average of 1 %, and the calcined synthesis product acquires a uniform structure of powder body of porous agglomerates up to 100 μm in size sintered from well-defined crystalline nanosized, and submicron ZnO particles with an average crystallite size of 40 nm. In the paper [11], nanostructured ZnO obtained for the first time by the solution SHS method was used as a photocatalyst for the phenol decomposition, in an aqueous solution under the action of electromagnetic radiation (ultraviolet and visible). In the calcined state, it showed high photocatalytic activity leading to near-complete phenol decomposition in 3.5–4.5 h of ultraviolet irradiation. However, under the action of visible light, the photocatalytic activity turned out to be significantly lower than under ultraviolet irradiation: after 5 h of irradiation with visible light, the phenol concentration decreased by only 10 % [11].

The work [11] did not study the grinding of the synthesized zinc oxide (SHS-S product), and the effect of grinding on the photocatalytic activity in the phenol decomposition. Such a study is of definite interest because an increase in the specific surface area of a heterogeneous catalyst during its grinding usually improves the catalysis efficiency; therefore, much attention is paid to increasing the zinc oxide dispersion and the use of ZnO nanoparticles in photocatalysis [2–4]. Another type of the SHS process for zinc oxide has not been studied either, when burning not a solution of the initial re-agents (SHS-S), but a gel from the initial dry mixture of the same re-agents (SHS-G). This process is implemented simpler and quicker and can lead to the ZnO synthesis with a higher photocatalytic activity in the phenol decomposition.

The aim of this study is to increase the photocatalytic activity of zinc oxide synthesized both by the SHS-S method when burning a solution of re-agents by grinding the combustion product in various ways, and by the SHS-G method by burning the gel from the initial dry mixture of the same re-agents.

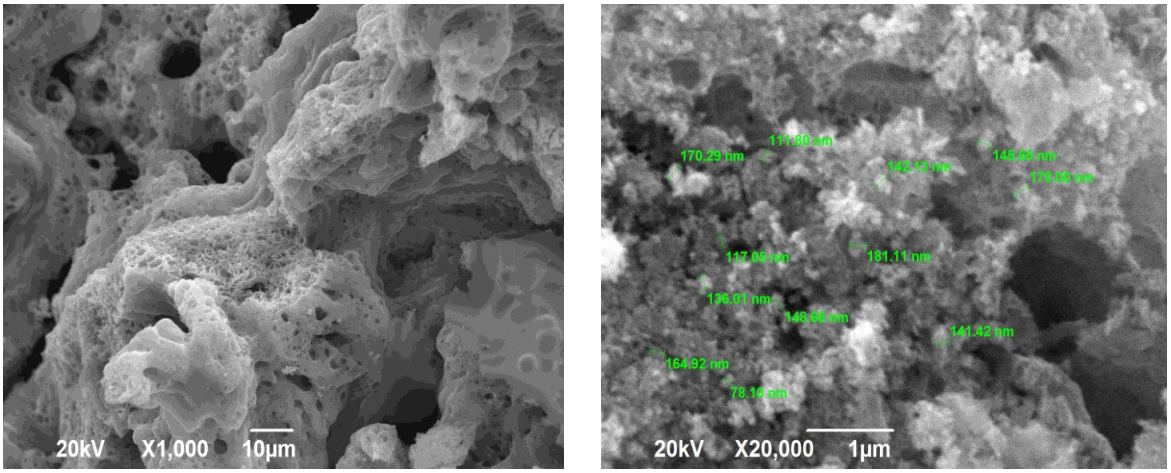

Fig. 2. *Microstructure of the solution combustion product at different magnifications at φ=2 [11, p. 936]*

METHODS

For the experimental studies, the following re-agents were used: zinc nitrate 6-aqueous $Zn(NO_3)_2 \cdot 6H_2O$ produced according to GOST 5106-77, of analytical grade; glycine $C_2H_5NO_2$ (GOST 5860-75, analytical grade); distilled water (GOST 6709-72); technical synthetic phenol (GOST 23519-93, high grade).

The equation for the ZnO synthesis reaction using the selected re-agents is written as [11]:

$$\mathrm{Zn(NO_3)_2} + \frac{10}{9}\varphi\,\mathrm{C_2H_5NO_2} + \frac{5}{2}(\varphi - 1)\,\mathrm{O_2} = \\ = \mathrm{ZnO} + \frac{25}{9}\varphi\,\mathrm{H_2O} + \frac{20}{9}\varphi\,\mathrm{CO_2} + \left(\frac{5}{9}\varphi + 1\right)\mathrm{N_2}, \quad (1)$$

where the dimensionless φ criterion characterizes the molar ratio of fuel and oxidizer.

At φ<1, the excess oxygen is released from the mixture of re-agents, and at φ>1, the oxygen required for the complete oxidation of elements is consumed from the surrounding gaseous medium. (Note that anhydrous zinc nitrate appears in equation (1), since when the mixture of re-agents is heated, almost all free and bound water evaporates, and the synthesis reaction proceeds during the combustion of an almost anhydrous gel [7].) The φ value largely determines a combustion mode, as well as the combustion product composition and structure. The experimental study of the combustion process and the combustion products was carried out with changing the values of the criterion φ in the range of 0.25≤φ≤3 with a step of 0.25.

Mixtures of re-agents were heated in a flat-bottomed metal vessel on an electric heater with a power of 1 kW. The average temperature of the contact metal surface of the electric heater was T_S=460 °C. When studying the SHS-S method, the volume of saturated aqueous solutions of mixtures of re-agents with V=25 ml and a height thickness of h=6.5 mm was used for heating.

The solution heating led to the spontaneous onset of a chemical reaction with intense heat and gas evolution (self-ignition), culminating in combustion of various types: 1) flameless combustion without the formation of luminous zones; 2) smoldering with the formation of focal and frontal luminous zones; 3) overall combustion with the formation of a flame. After the end of combustion, a loose or dense sinter of solid combustion products remained in the vessel, the mass of which depended on the combustion type. Intense combustion could lead to the release of a part of the reacting mixture and combustion products from the vessel, so that only a part of the combustion products remained in the vessel. In this regard, the authors calculated the product mass conservation coefficient K_M as the ratio of the mass of the combustion product remained in the reaction vessel after the experiment, to the theoretical product mass calculated according to the reaction equation. Along with determining the combustion type and calculating the K_M coefficient, the combustion time characteristics were determined: 1) the delay time for the onset of combustion (ignition) from the start of heating; 2) the combustion duration. One should note that the specified time characteristics of combustion and the product mass conservation coefficient K_M were first introduced when considering the solution SHS process and studied in our work [11].

When studying the SHS-G process, the authors used the masses of mixtures of dry re-agents corresponding to the mass of mixtures of re-agents in a saturated aqueous solution with a volume of V=25 ml at the corresponding φ value. Dry powders of the components – zinc nitrate and glycine – were weighed and mixed manually in a mortar until visually homogeneous. During mixing, the mixture of powders was saturated with moisture from the air due to hygroscopicity to form a gel, which was placed in a metal flat-bottomed vessel for heating on an electric heater with a surface temperature of T_S=460 °C. Heating led to spontaneous gel ignition, the occurrence of the SHS-G process in the form of combustion, and the formation of a combustion product – zinc oxide with impurities of products of incomplete combustion, mainly in the form of free and combined carbon.

To remove impurities of free carbon and carbon bound with oxygen and hydrogen in the unburned fuel residues, the combustion product was subjected to calcination (oxidizing burning) in the NAKAL PL 5/12.5 muffle furnace with an air atmosphere at a temperature of 500, 650, and 750 °C during 1 h.

X-ray diffraction (XRD) phase analysis of combustion products was carried out on an ARL X'TRA Thermo Fisher Scientific X-ray diffractometer. The microstructure and elemental chemical composition were studied using a JSM-6390A scanning electron microscope (Jeol) with a JSM-2200 energy dispersive spectroscopy (EDS) device. The size of coherent scattering regions (CSRs) was estimated using the Scherrer formula.

Grinding of the solution SHS powdered product (SHS-S product) was carried out in three ways. The first method – in a drum ball mill (DBM) with a volume of 1 l and a drum rotation speed of 120 rpm, 1 kg of milling agents in the form of rollers with a diameter of 5 mm made of ШХ15 steel and up to 7 g of grindable powder were loaded. The grinding time was 15, 30, and 60 min. The second method is grinding in an Activator-2SL planetary-centrifugal mill (PCM). Grinding balls with a diameter of 5 mm and a mass of 375 g made of ШХ15 steel and up to 7 g of grindable powder were loaded into two drums with a volume of 270 ml each with an inner radius of 35 mm. The drums were mounted on a planetary disk with a ratio of the radii of rotation of the disk and drums equal to 1.5, and ensured grinding at a centrifugal acceleration of 20 g. The powder grinding time in the PCM was 15, 30, and 45 s. The third way – the synthesized powder was manually ground with a pestle in a ceramic mortar with a grinding time of 5, 10, and 15 min.

The synthesized ZnO photocatalytic activity was studied by decomposition of phenol dissolved in 100 ml of water at a concentration of 1 mg/l. ZnO particles were dispersed in the solution in an amount of 1 g/l using a Sapphire UZV-2.8 ultrasonic bath. The photocatalytic decomposition process proceeded with constant stirring of the solution under the action of ultraviolet radiation with a wavelength of 365 nm on a Lab 365 nm TL-D 18W BLB device from Philips. The concentration of phenol dissolved in water was determined by registering a characteristic fluorescent peak by the spectrofluorimetry method using a Shimadzu RF-6000 device. (SHS-G and SHS-S products for comparative studies of their photocatalytic activity after synthesis or calcination were subjected to grinding during 10 min in a ceramic mortar.)

RESULTS

SHS-S product grinding

Fig. 3 shows the appearance of the ground non-calcined combustion product synthesized from a solution of zinc nitrate with glycine at φ=2 after grinding in a drum ball mill (60 min) and a mortar (15 min).

Fig. 3 demonstrates that the appearance of the synthesized combustion product at the end of grinding in a DBM and in a mortar vary notably. If in a ball mill the ground product sticks by a continuous layer on the grinding agents (steel rollers), and on the steel wall of the drum (Fig. 3 a), then in a ceramic mortar the sticking of the product is much less (Fig. 3 b). Significant sticking of the ground product was also noted during intensive grinding in a planetary mill. Such ground product sticking in the DBM and PCM takes a significant part of the product. After each grinding session, it is necessary to clean and wash the drums and grinding agents (rollers and balls) from sticky product, to dry them, which leads to great inconvenience. Moreover, when grinding in a DBM and PCM, the powder darkens, which indicates its possible contamination with the material of the grinding agents. With much simpler grinding in a mortar, there is practically no sticking of the powder, and it does not darken during grinding.

The microstructure of the non-calcined combustion product ground by all three methods is represented in Fig. 4. The time of grinding in a mortar was 10 min, in DBM – 60 min, in PCM – 45 s.

The microstructure of the powder ground by different ways also varies markedly (Fig. 4). After grinding in a mortar (Fig. 4 a), the powder structure is quite homogeneous and consists of submicron agglomerates of smaller particles with a visually observed minimum size of 60 to 90 nm. After grinding in a ball mill (Fig. 4 b), the structure of the ground material is heterogeneous and consists of a mixture of individual small particles with a visually observed minimum size of 70 to 140 nm and agglomerates, the size of which reaches 3 μm.

Increasing the time of grinding in the DBM leads to a decrease in the number of individual small particles, and an increase in the number and size of particle agglomerates with an amorphous component between them. In a planetary mill, the ground material acquires a more heterogeneous structure (Fig. 4 c). There are practically no individual small particles with a minimum size of 150 to 250 nm, the powder consists of a pasty mass of micron-sized agglomerates with an amorphous component. Increasing the grinding time also leads to coarsening of the agglomerates.

The phase composition of the non-calcined synthesis product ground by all three methods is shown in Fig. 5 and in Table 1.

A quantitative X-ray diffraction analysis, according to X-ray diffraction patterns (Fig. 5 and Table 1) of the ground non-calcined combustion product, shows the content of both carbon impurity from 2 to 10 % and a significant content of Fe_2O_3 iron oxide impurity: 30 % after grinding in the DBM and 36 % after grinding in the PCM, and the absence of this impurity after grinding in a mortar. Thus, intensive milling of ZnO powder in the DBM and PCM actually leads to powder contamination with an admixture of iron oxide from steel drums and grinding agents, but in the case of grinding in a ceramic mortar, there is no such contamination.

The product synthesized from a solution of zinc nitrate with glycine at φ=2 was also ground after oxidative roasting (calcination) at 650 °C during 1 h. Fig. 6 presents the results of grinding the calcined product in various ways. The time of grinding in the mortar was 15 min, in the DBM – 60 min, and in the PCM – 45 s.

a ***b***

Fig. 3. *The appearance of the non-calcined solution combustion (SHS-S) product after grinding:* ***a*** *– in the drum ball mill;* ***b*** *– in the mortar*

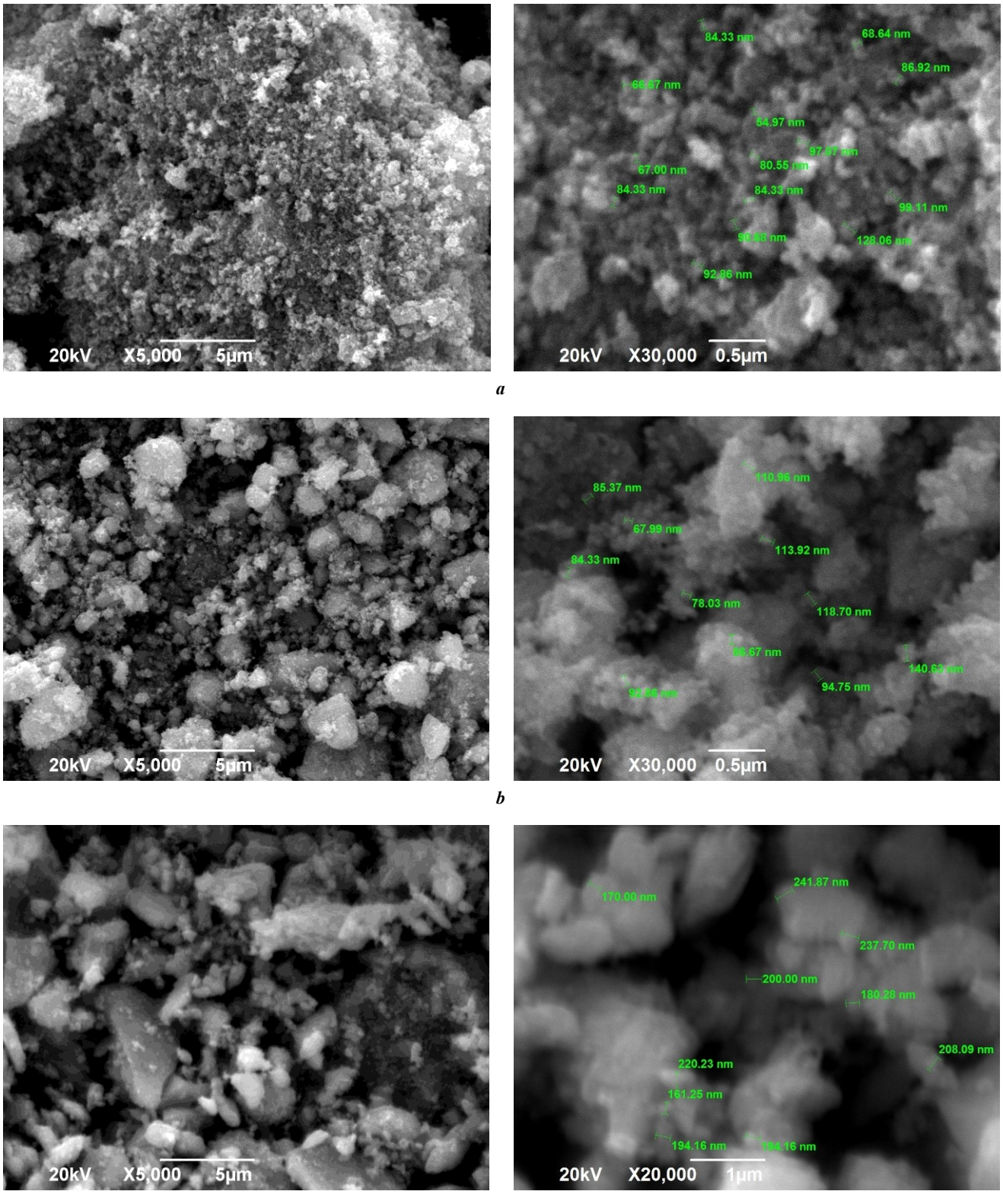

Fig. 4. *Microstructure of the non-calcined solution combustion (SHS-S) product after grinding:* ***a*** *– in the mortar;* ***b*** *– in the drum ball mill;* ***c*** *– in the planetary-centrifugal mill*

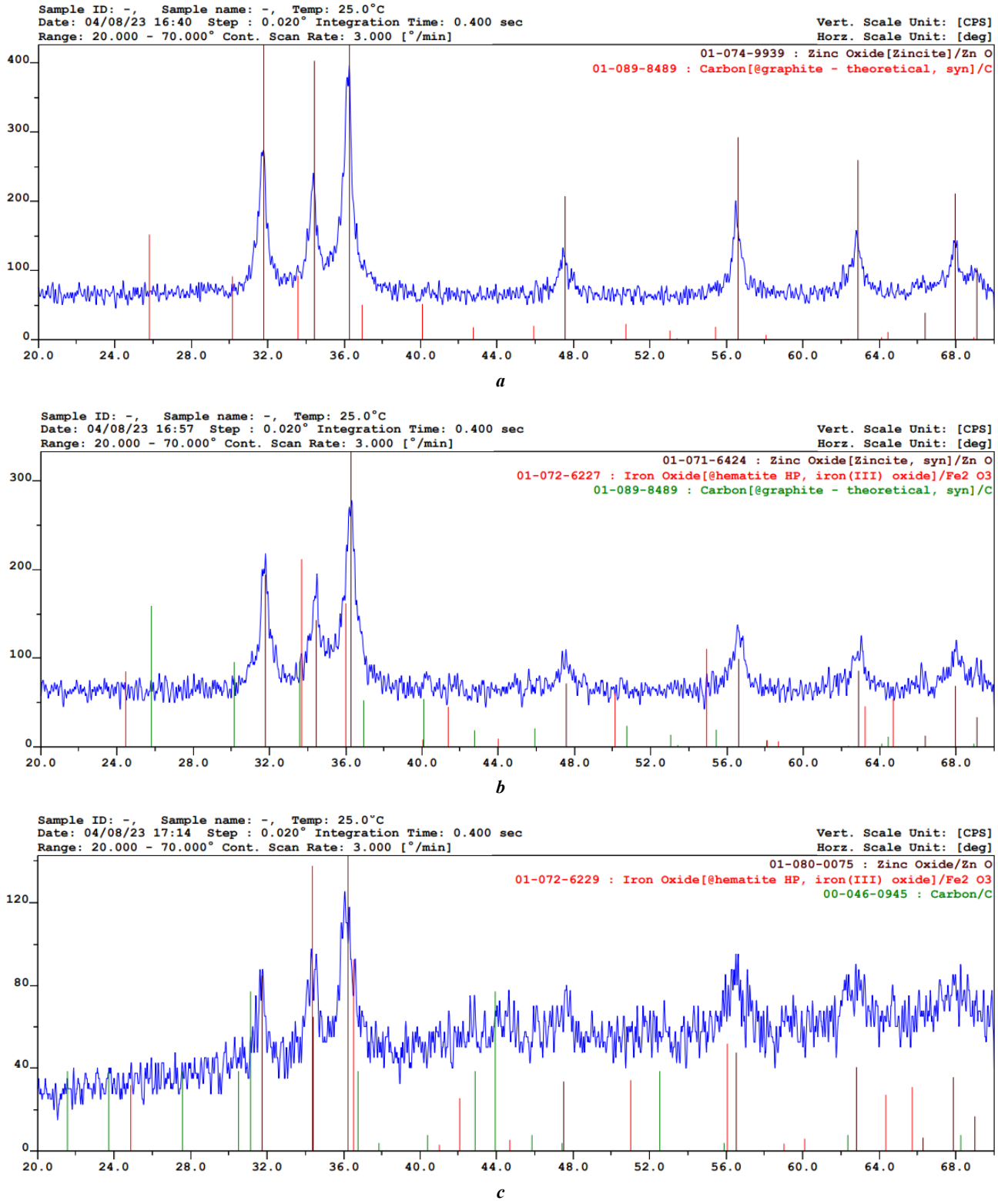

Fig. 5. *XRD pattern of the non-calcined solution combustion (SHS-S) product after grinding:* ***a*** *– in the mortar;* ***b*** *– in the drum ball mill;* ***c*** *– in the planetary-centrifugal mill*

Table 1. *Phase composition of the non-calcined solution combustion (SHS-S) product at different grinding methods*

Type of grinding	Content, %		
	ZnO	**C**	**Fe_2O_3**
A mortar, 15 min	93	7	0
A drum ball mill, 60 min	60	10	30
A planetary-centrifugal mill, 45 s	62	2	36

Fig. 6 demonstrates that the amorphous component from the residues of unburned fuel in the structure is absent. The most uniform and fine powder structure is observed after grinding in a mortar. This is confirmed by the results of determining the particle-size distribution of the combustion product calcined at 650 °C during 1 h after grinding in a mortar and PCM (Fig. 7) with an average particle size of D_{50}=0.90 and 8.27 μm, respectively.

Fig. 7 clearly shows that after grinding in a mortar, the particle size is in the range from 0.18 to 8.3 μm, and after grinding in a planetary mill – from 0.18 to 130 μm. The lower limits and submicron sizes here refer to individual small particles, and micron sizes up to the upper limits refer to strong sintered porous agglomerates of submicron ZnO particles that are not separated by ultrasonic treatment in water [11].

Fig. 8 presents the elemental chemical composition of the calcined combustion product determined by the EDS method after milling by various methods. The time of grinding in a mortar was 10 min, in a DBM – 60 min, in a PCM – 45 s.

The local elemental composition of the calcined combustion product after grinding (Fig. 8) shows the presence of carbon residues ranging from 0.83 to 2.01 % after grinding by all methods, but the presence of iron impurities was found only after grinding in mills: 2.07–6.38 % (DBM) and 0.8–2.4 % (PCM).

Based on the results obtained, one can conclude that simple grinding in a mortar gives the purest and finest ZnO powder obtained by the SHS-S method.

SHS-S product photocatalytic activity

Fig. 9 presents the results of the application of the non-calcined SHS-S product ground in a drum ball mill and a mortar for the phenol photocatalytic decomposition in an aqueous solution under the action of ultraviolet irradiation.

Fig. 9 shows that, regardless of the duration of grinding in a DBM, the phenol concentration behaves much the same – during the entire 5.5 h of irradiation, it fluctuates around the initial relative value of 100 % without a noticeable decrease, and even vice versa, with an increase of up to 20 % against the initial value.

The results of studying the phenol photocatalytic decomposition using the combustion product ground by different methods and calcined for 1 h at different temperatures (500, 650, and 750 °C) are shown in Fig. 10.

It is obvious that the selected calcination temperatures give similar results, while different grinding methods lead to significantly different results. Calcined ZnO powder ground in a mortar has a much higher photocatalytic activity than one ground in ball and planetary mills. Judging by the data in Fig. 8 about the local content of elements in ZnO powder, all these three powders have approximately the same small carbon impurities (in the range of 1–2 %), but the powder after grinding in a mortar does not have iron Fe impurities and, after grinding in mills, iron contamination is more noticeable: from 2.07 to 6.38 % in a DBM and from 0.8 to 2.4 % in a PCM. Moreover, Fig. 6 and 7 show that when grinding in a mortar, the powder is much finer than when grinding in mills, in particular, the average particle size D_{50}=0.90 μm when grinding in a mortar and D_{50}=8.27 μm after a PCM. Thus, when grinding the calcined solution SHS product in a mortar, the obtained ZnO powder is much purer and finer than when grinding in ball and planetary mills. This explains the highest photocatalytic activity of ZnO powder ground in a mortar in the reaction of phenol decomposition in an aqueous solution under the action of ultraviolet irradiation (Fig. 10).

Obtaining SHS-G product

During heating, convective mixing of the viscous gel was observed, and after some time a combustion reaction spontaneously began, the duration of which determined the combustion time. Fig. 11 demonstrates the dependence of the mass conservation coefficient of the product of the combustion in the K_M vessel on the φ criterion in the range of $0.25 \le \varphi \le 3$ for this SHS-G process obtained as a result of three experiments for each value of the φ criterion.

When comparing Fig. 11 (for the SHS-G process with gel combustion) with a similar Fig. 1 (for the SHS-S process with solution combustion), one can observe that they are close and indicate the existence of an explosive combustion mode with an almost complete release of the combustion product from the reaction vessel in the range of molar ratios of glycine with zinc nitrate in the initial mixture of re-agents of $0.5 \le \varphi \le 1.5$. In the range of $\varphi > 1.5$, the K_M mass conservation coefficient of the SHS-G product tends to the K_M=1 value with an increase in the φ criterion up to the value of φ=3. By comparison, in the case of the SHS-S product, the K_M coefficient tended to the K_M=1.5 value, which is an indication of greater contamination of the SHS-S product with the unburned glycine fuel residues. For both the SHS-G and SHS-S processes, the ignition delay time differs significantly. In the case of using dry mixtures of re-agents, combustion begins much faster (1.5 min on average) than in the case of dissolved

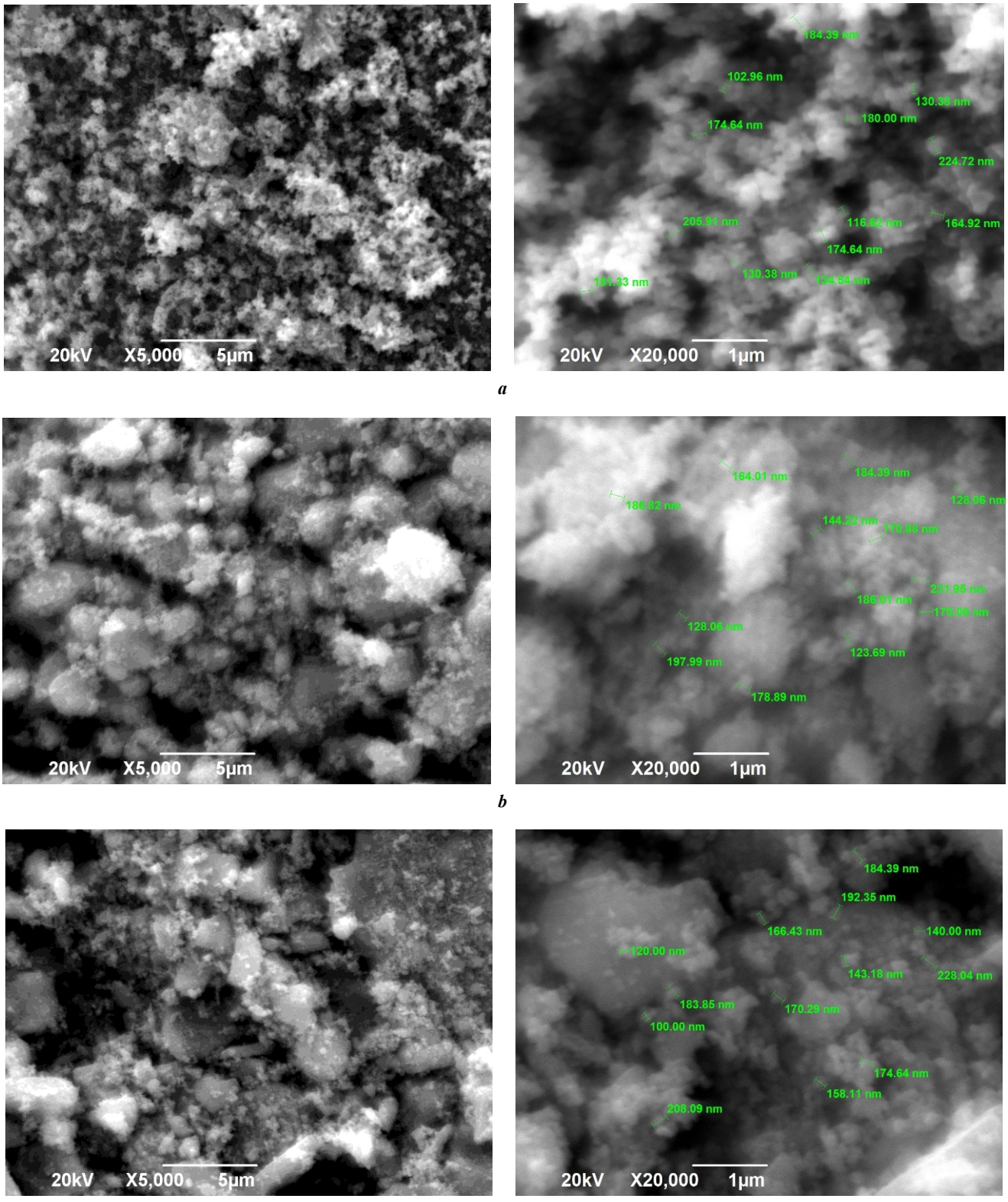

a

b

c

Fig. 6. *Microstructure of the calcined solution combustion (SHS-S) product after grinding:* ***a*** *– in the mortar;* ***b*** *– in the drum ball mill;* ***c*** *– in the planetary-centrifugal mill*

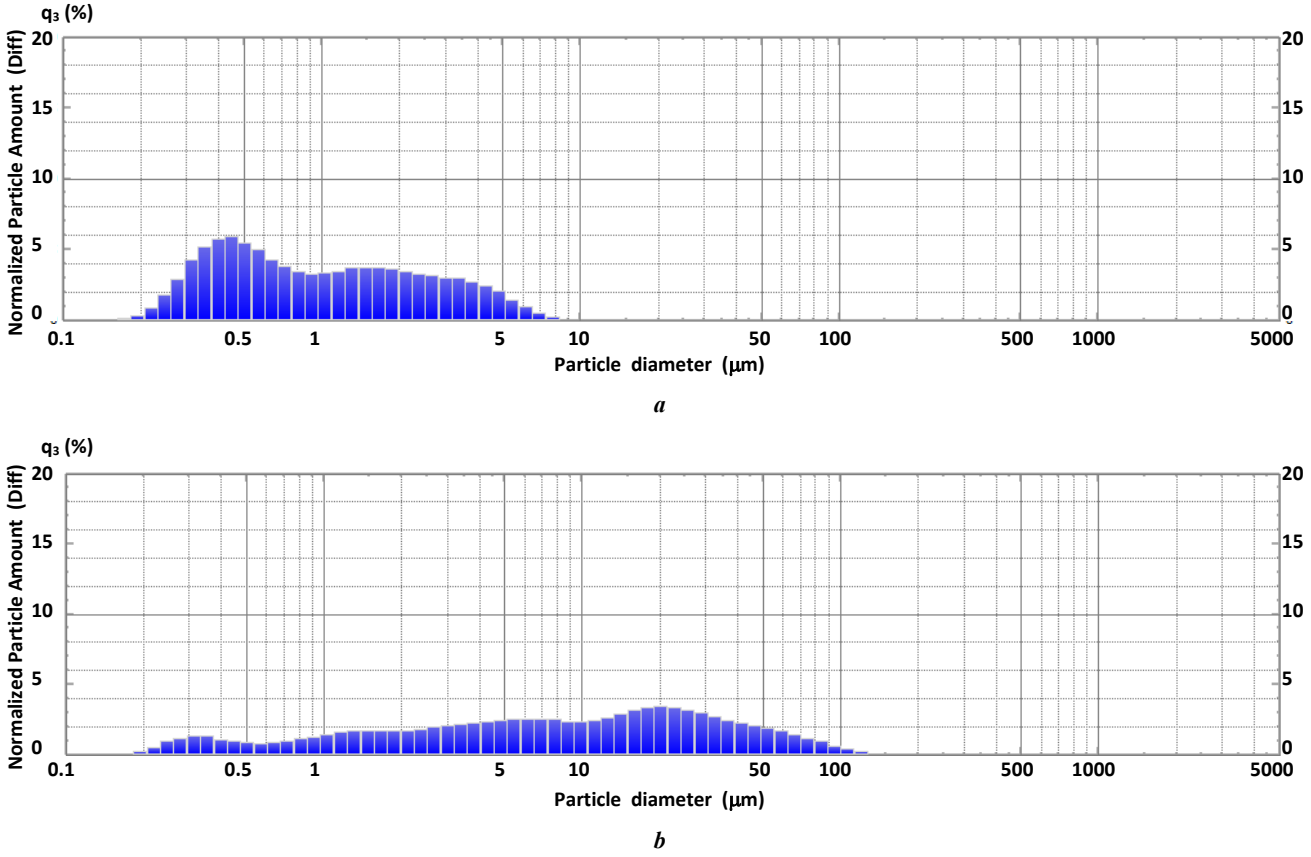

Fig. 7. *The particle-size distribution (the dependence of the normalized particle amount q_3 (%) on the particle diameter) of the powdered calcined solution combustion (SHS-S) product after grinding:* ***a*** *– in the mortar, D_{50} = 0.90 µm;* ***b*** *– in the planetary-centrifugal mill, D_{50} = 8.27 µm*

re-agents (8 min on average), since in the latter case a lot of time is spent for heating the solution to boiling water and evaporating water before gel formation. The time and type of combustion, color and consistency of the synthesized ZnO combustion product in the SHS-G process remain close to those of the process and product of SHS-S[1].

Composition and structure of the SHS-G products

Fig. 12 and 13 show the results of determining the phase composition and microstructure of non-calcined SHS-G products for three different values of φ criterion: 0.25, 1, and 2.

Fig. 14 shows an example of determining the local content of elements at various points of the synthesized product by the EDS method.

The results of the XRD analysis of the SHS-G product at a minimum value of φ=0.25 show (Fig. 12 a) that the synthesis product consists of two phases: crystalline zinc oxide ZnO and free X-ray contrast carbon C with a graphite crystal lattice. The presence of free carbon indicates that the reaction temperature was not high enough to complete the chemical reaction of glycine oxidation. High peaks relative to the main background of the diffraction pattern indicate the presence of a formed crystal structure of wurtzite in zinc oxide obtained as a result of synthesis. The crystallite size obtained by the CSR assessment according to the Scherrer formula is 48, 41, and 40 nm on three peaks with the highest intensity, and the average crystallite size is 43 nm. Fig. 13 a demonstrates that the resulting powder has a homogeneous structure with non-agglomerated, clearly defined particles of equiaxial submicron crystals. It can be concluded that a highly dispersed powder with a particle size of less than 1 µm consisting of a mixture of nanosized and submicron particles with an average crystallite size of 43 nm has been synthesized.

Fig. 14 shows the results of the EDS analysis of the local elemental composition of this powder at three points. The results show a content of 0.83 to 1.77 wt. % of carbon in the combustion product, on average 1.18 %, which corresponds to the XRD results (Fig. 12 a) on the presence of free carbon in the product. The average values of carbon impurity in the non-calcined SHS-G product determined by the EDS method are equal to 1.45 and 1.9 % for the values of φ=1 and 2, respectively.

At φ=1, the synthesis product consists of two phases as well: crystalline ZnO and X-ray contrast carbon C. The average size of ZnO crystallites according to the Scherrer formula is 21 nm. A smoother transition of the diffraction pattern (Fig. 12 b) from the main background level to the peak level may indicate the appearance of an amorphous component in the synthesis products.

[1] *Novikov V.A., Titov A.A., Kryukov N.A., Kachkin E.M. Combustion modes of gel of zinc nitrate with various fuels in the synthesis of zinc oxide nanopowders. Sovremennye materialy, tekhnika i tekhnologii, 2022, no. 2, pp. 17–39. EDN: LFWVFA.*

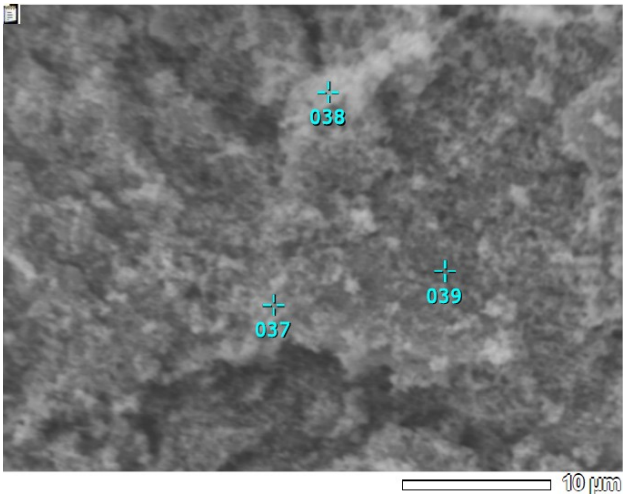

Element	Mass content, %, at the points		
	037	038	039
C	0.83	1.14	0.86
O	6.63	7.77	6.43
Zn	92.54	91.09	92.71

a

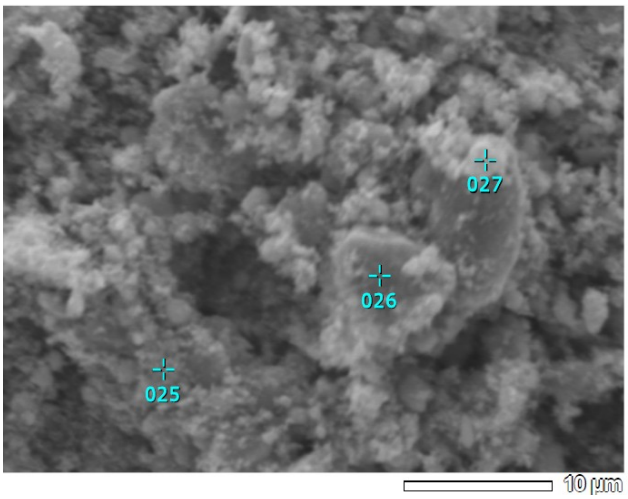

Element	Mass content, %, at the points		
	25	26	27
C	0.76	1.07	2.01
O	5.83	9.32	15.20
Fe	6.38	2.07	4.01
Zn	87.03	87.54	78.78

b

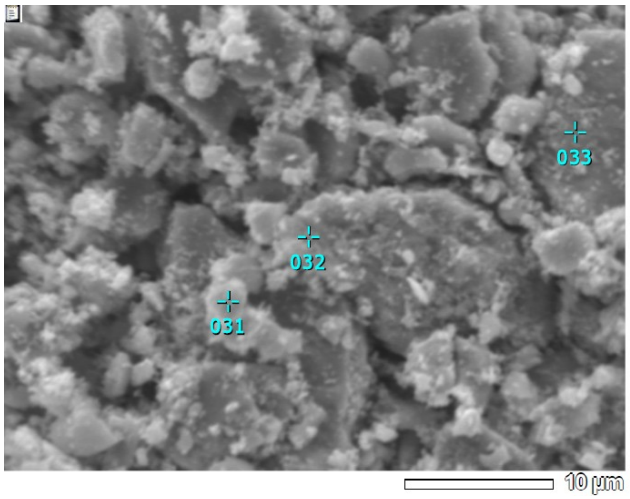

Element	Mass content, %, at the points		
	31	32	33
C	1.7	1.99	0.66
O	10.86	13.13	5.57
Fe	2.40	0.80	1.22
Zn	85.05	84.08	92.54

c

Fig. 8. *The local elemental composition of the calcined solution combustion (SHS-S) product after grinding:* ***a*** *– in the mortar;* ***b*** *– in the drum ball mill;* ***c*** *– in the planetary-centrifugal mill*

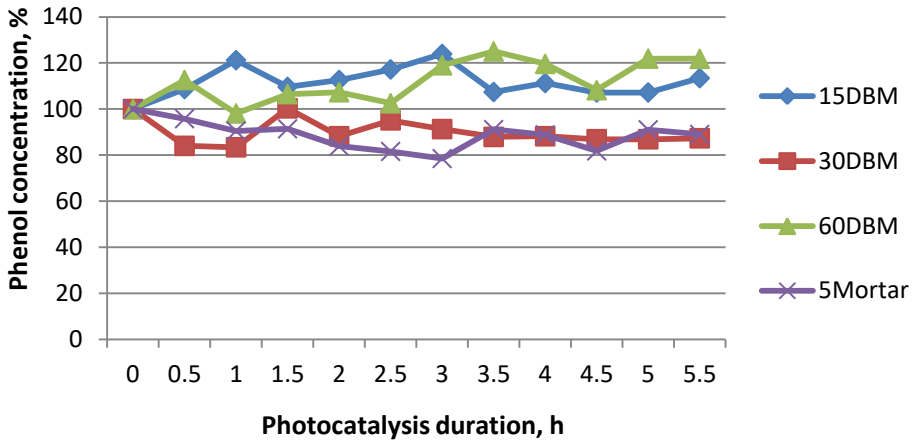

Fig. 9. *Change in time under the action of ultraviolet irradiation of the phenol relative concentration in an aqueous solution with a suspension of particles of the non-calcined solution combustion (SHS-S) product ground in the drum ball mill (15, 30, and 60 min) and in the mortar (5 min)*

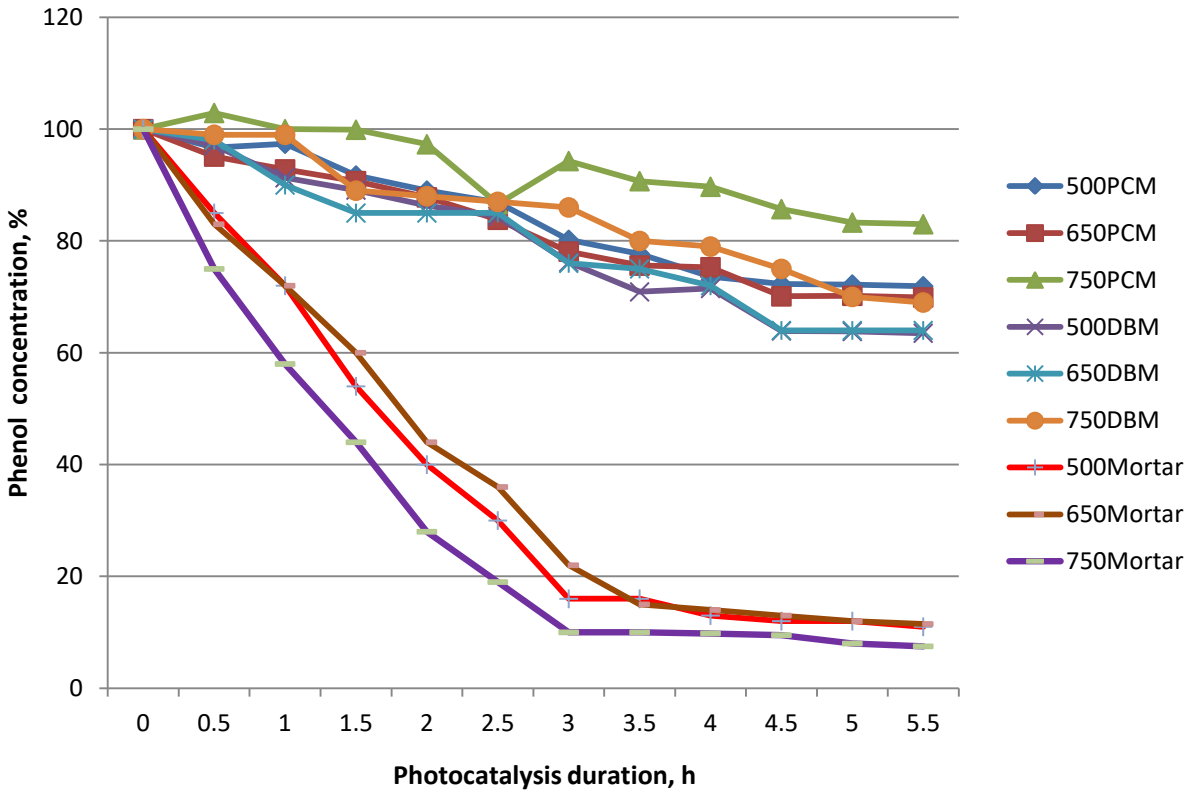

Fig. 10. *Change in time under the action of ultraviolet irradiation of the phenol relative concentration in an aqueous solution with a suspension of particles of the solution combustion (SHS-S) product calcined at different temperatures (figures for lines, °C) and ground in the mortar (10 min), in the drum ball mill (DBM) (30 min); and in the planetary-centrifugal mill (PCM) (45 s)*

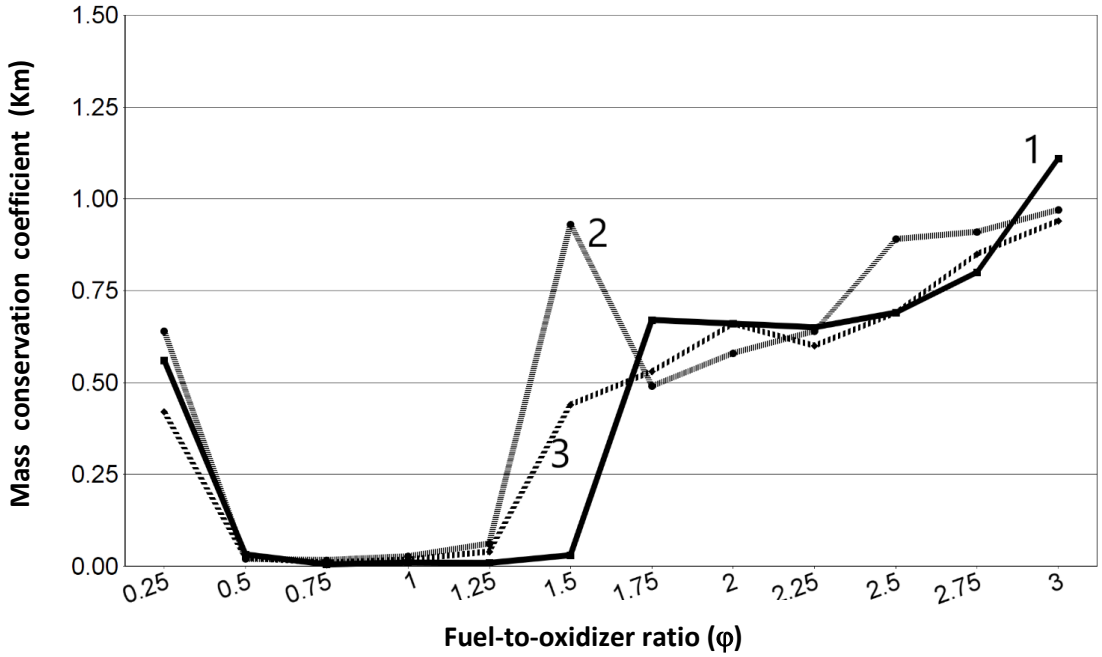

Fig. 11. *The dependence of the product mass conservation coefficient K_M on the value of the criterion φ at the combustion of gel from dry reagents (SHS-G). The numbers on the lines indicate the numbers of experiments*

This is confirmed by the structure of the synthesized product in the form of a frozen foamy mass with many pores of various diameters and agglomerates of small submicron oval particles (Fig. 13 b). Local elemental analysis of the combustion product gives an average carbon content of 1.45 wt. %.

With a further increase in φ, the microstructure of the combustion product remains similar – in the form of a frozen melted amorphous foam with many pores of various diameters and agglomerates of small nanosized and submicron particles (Fig. 13 c). The diffraction pattern (Fig. 12 c) for φ=2 shows the presence of only the ZnO crystalline phase with an average crystallite size of 34 nm. At the same time, from the results of the EDS analysis of this SHS-G product, it follows that the content of carbon impurities in it is on average 1.9 %, which indicates the presence of carbon in the form of an impurity of free carbon in amorphous form and in the form of combined carbon in the unburned fuel residues. The EDS analysis of a similar SHS-S product synthesized at φ=2 showed a significantly higher average carbon content – about 10 % [11]. From the comparison of carbon content in the SHS-G and SHS-S products synthesized at other φ values, the general conclusion follows that the carbon impurity content in the non-calcined SHS-G products is significantly lower in comparison with the non-calcined SHS-S products synthesized at the same values of φ criterion.

The results of determining the carbon impurity in the SHS-G product after calcination (oxidative annealing) at a temperature of 650 °C during 1 h (φ=2) are shown in Fig. 15 and equal on average to 0.94 %.

Thus, calcination noticeably reduces the carbon impurity content in the SHS-G product from 1.9 % for the non-calcined product at φ=2 to 0.94 % (Fig. 15).

Photocatalytic activity of the synthesized products

Fig. 16 presents the results of comparing the photocatalytic activity for non-calcined synthesis products obtained in the SHS-S and SHS-G modes with different fuel/oxidizer ratios in the composition of the initial reaction mixture, i.e., with different φ criterion values: 0.25, 1, and 2.

Fig. 16 shows that for all φ values, in the first hours of ultraviolet irradiation, the SHS-G products exhibit slightly higher catalytic activity, which is close to the activity of the SHS-S products for the same φ value, but after 5 h of irradiation, their activity practically coincides. In general, the photocatalytic activity of non-calcined products is low, especially at φ=2, and leads to a decrease in the phenol concentration in an aqueous solution by 40–60 % over 5 h of irradiation. These results can be explained by the fact that non-calcined SHS-G products are slightly purer in terms of the carbon impurity content than non-calcined SHS-S products. At φ=2, the carbon impurity content is the highest compared to φ=0.25 and 1, and the smallest ZnO crystallite size of 21 nm (Fig. 12) is observed at φ=1 with the highest photocatalytic activity.

Fig. 17 shows the results of the same comparison for the SHS-S and SHS-G products calcined for 1 h at 650 °C.

The authors also determined the particle-size composition of these calcined and ground in a mortar (10 min) SHS-G products synthesized at various φ values (Fig. 18).

As one can see from Fig. 17, calcination (650 °C, 1 h) of the synthesized SHS-S and SHS-G products significantly increases their photocatalytic activity, especially of the SHS-G products, which contribute to the almost complete phenol decomposition in 3.5–4.5 h of ultraviolet irradiation. Such activity of the products is explained both by their significant purification from carbon impurities during calcination to a level of 1 % ([11] and Fig. 15) and by

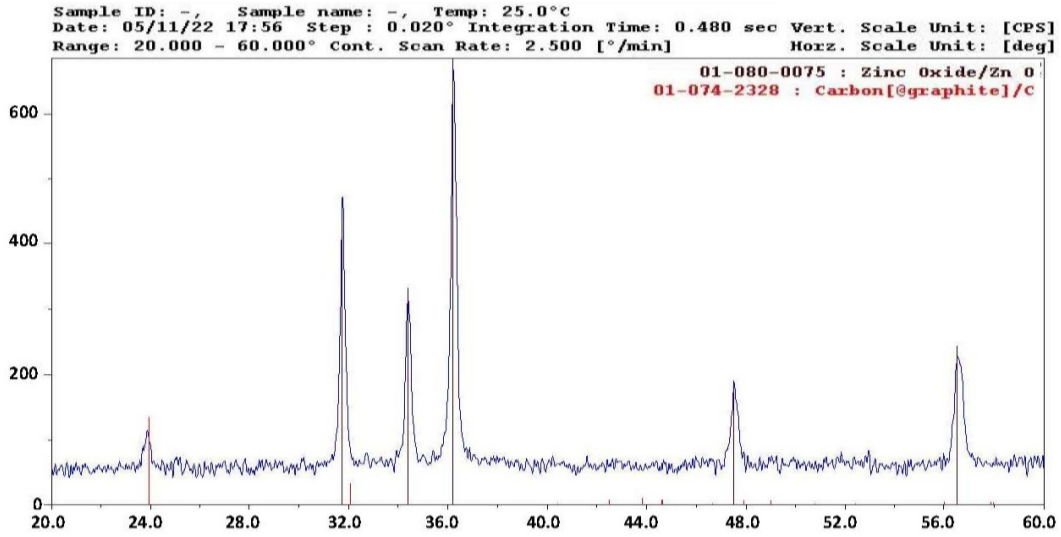

a

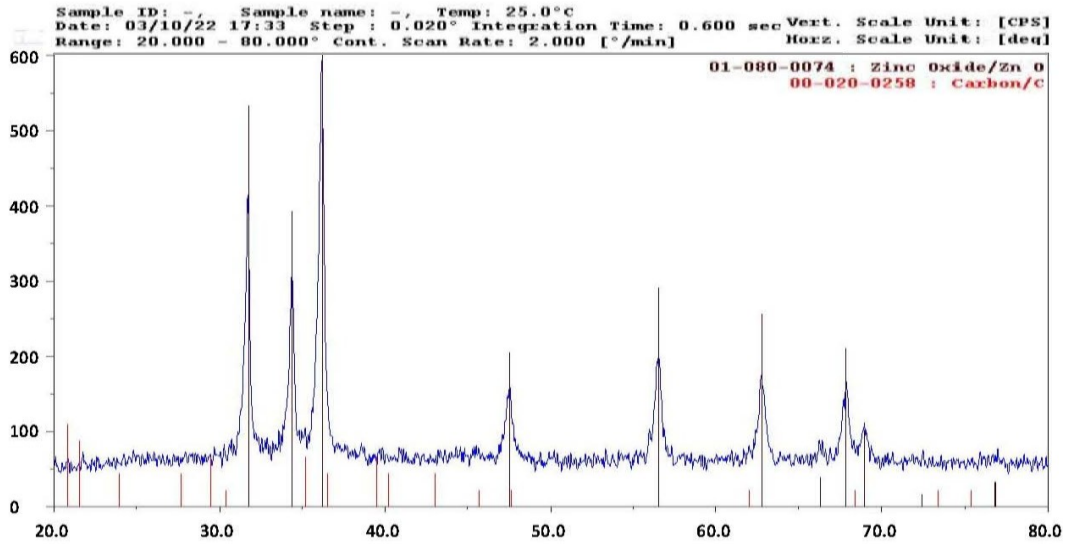

b

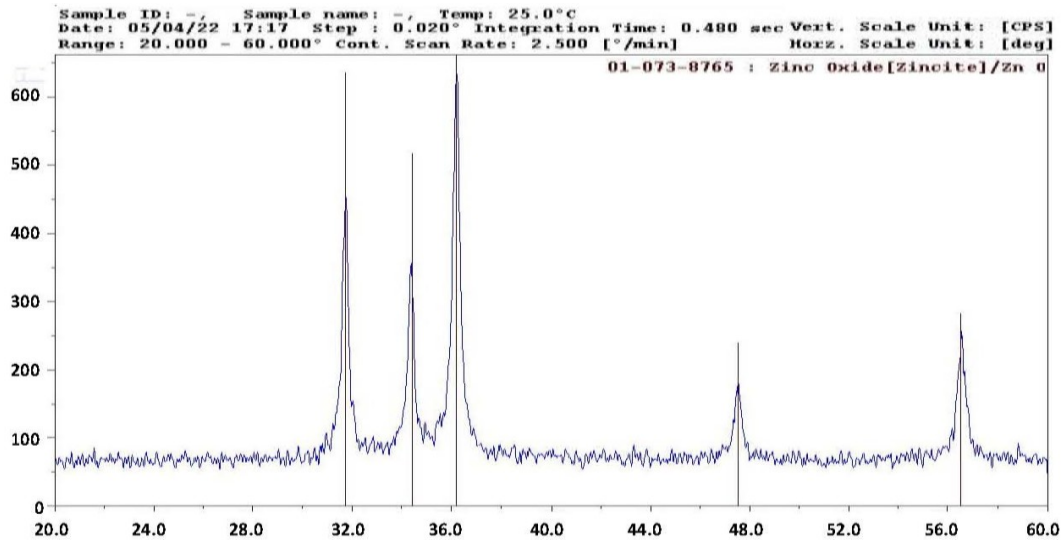

c

Fig. 12. *XRD patterns of the non-calcined gel combustion (SHS-G) product at various φ:* ***a*** *– φ=0.25;* ***b*** *– φ=1;* ***c*** *– φ=2*

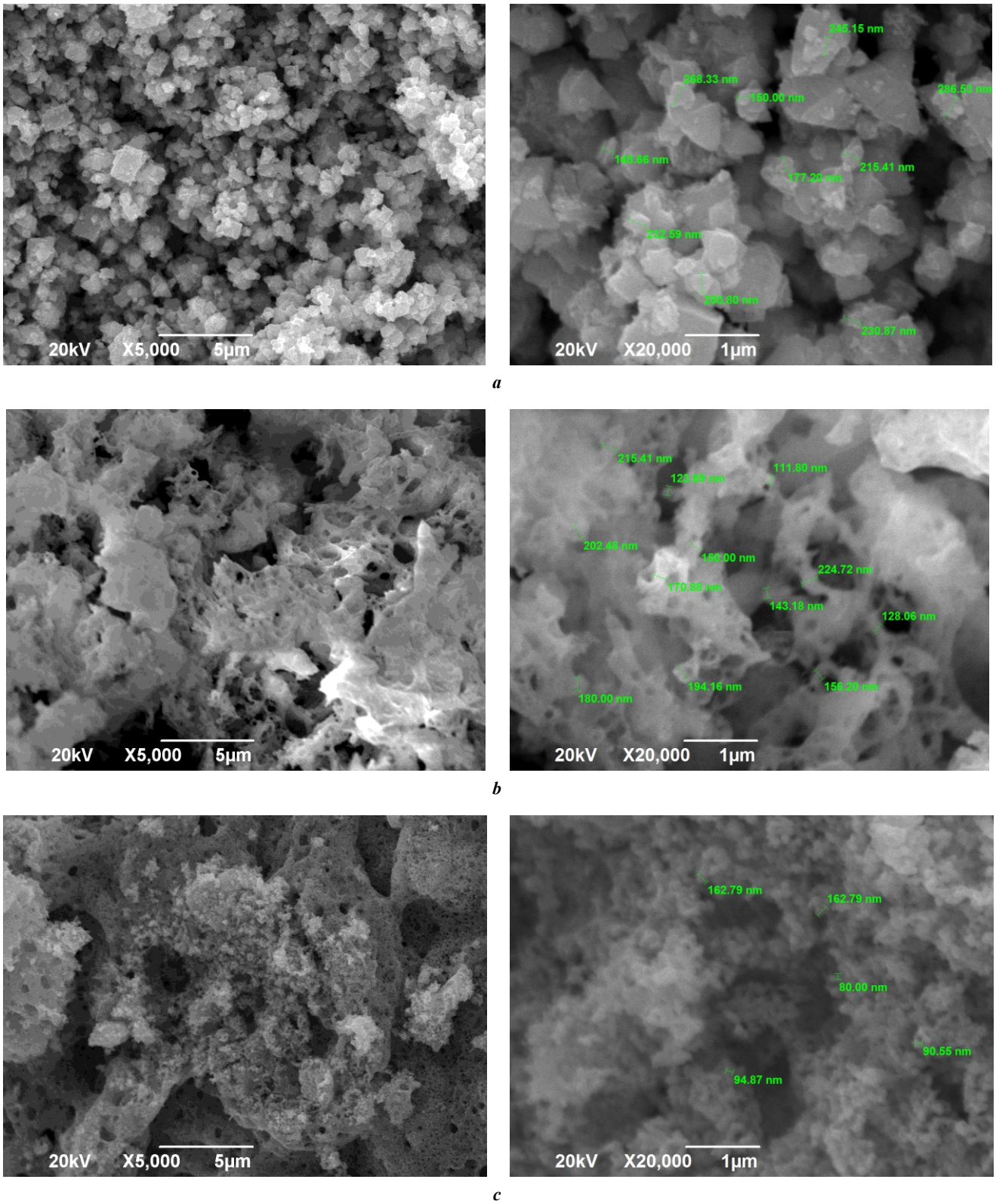

Fig. 13. *Microstructure of the non-calcined gel combustion (SHS-G) product at various φ:* ***a*** *– φ=0.25;* ***b*** *– φ=1;* ***c*** *– φ=2*

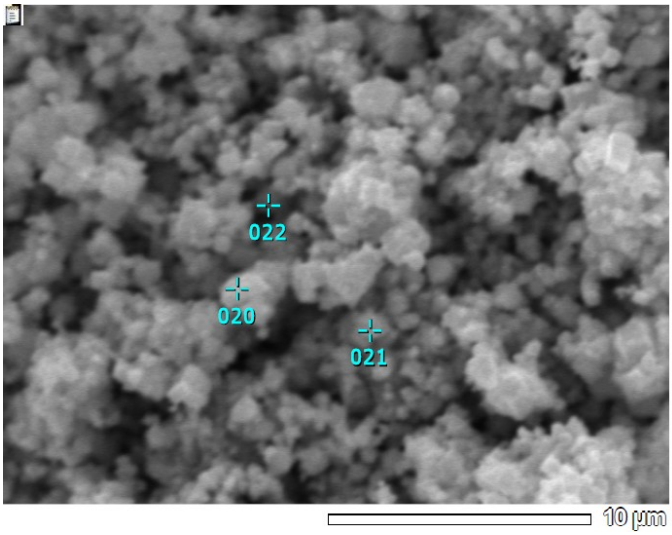

Element	Mass content, %, at the points		
	20	21	22
C	1.77	0.95	0.83
O	13.95	6.02	6.73
Zn	84.29	93.03	92.44

Fig. 14. *The local elemental composition of the non-calcined gel combustion (SHS-G) product at φ=0.25*

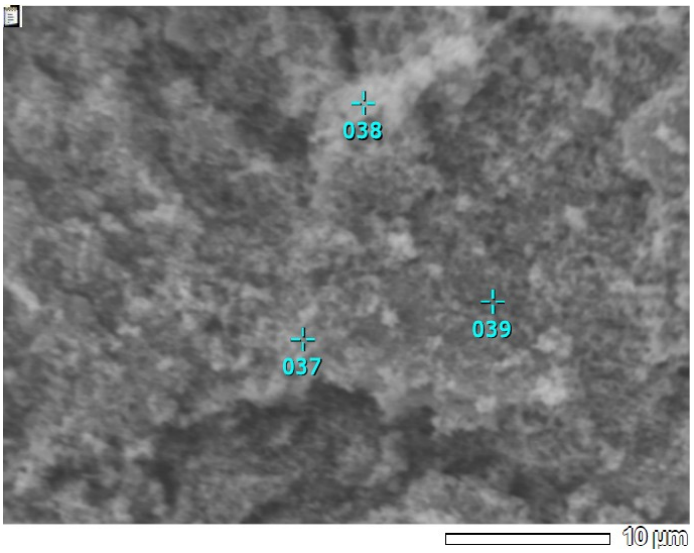

Element	Mass content, %, at the points		
	037	038	039
C	0.83	1.14	0.86
O	6.63	7.77	6.43
Zn	92.54	91.09	92.71

Fig. 15. *The local elemental composition of the calcined gel combustion (SHS-G) product at φ=2*

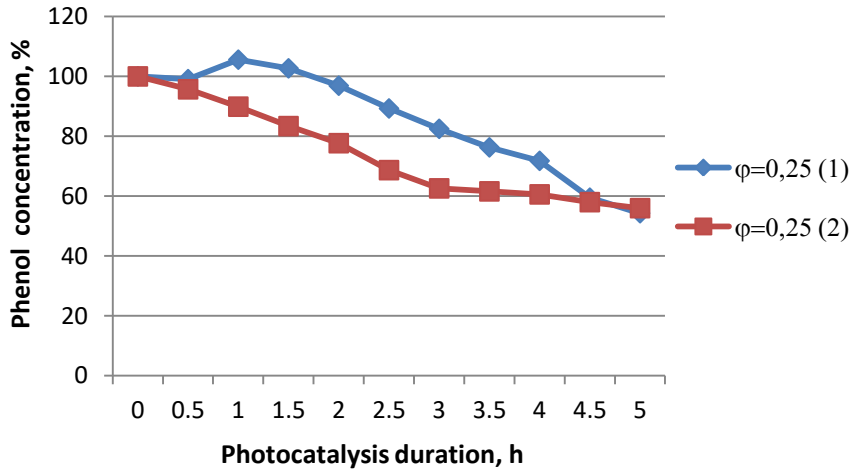

a

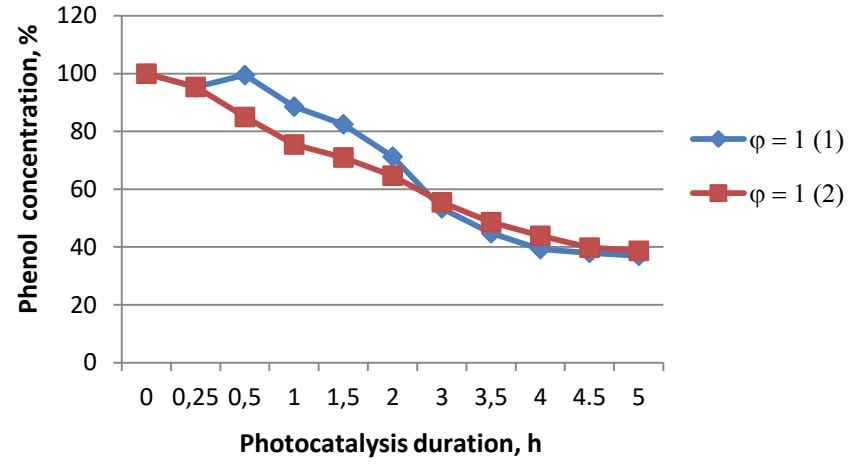

b

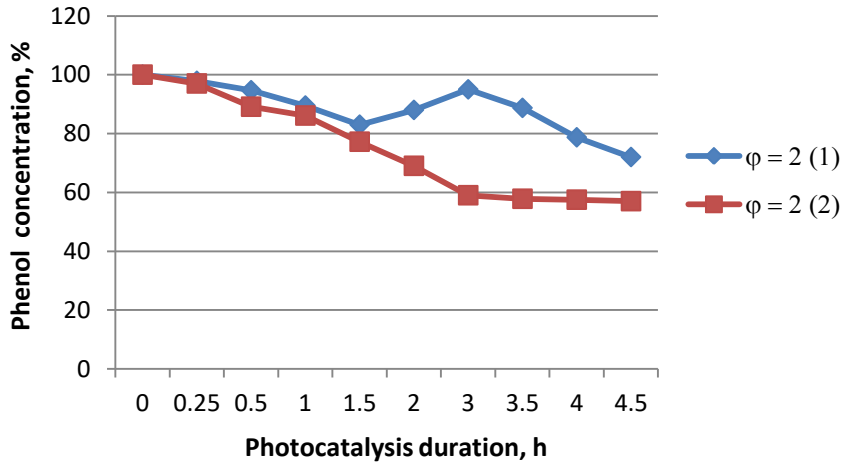

c

Fig. 16. *Change in time under the action of ultraviolet irradiation of the phenol relative concentration in an aqueous solution with a suspension of particles of non-calcined products of solution combustion (SHS-S) (1) and gel combustion (SHS-G) (2) synthesized at:*
a *– φ=0.25;* ***b*** *– φ=1;* ***c*** *– φ=2*

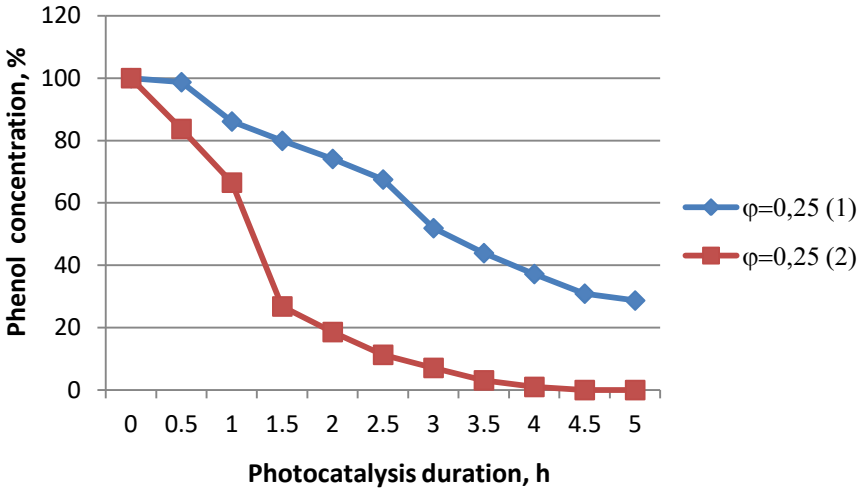

a

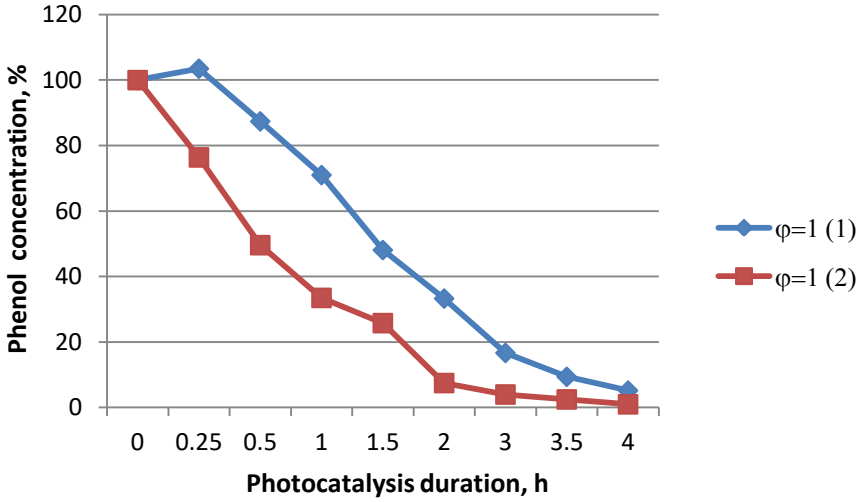

b

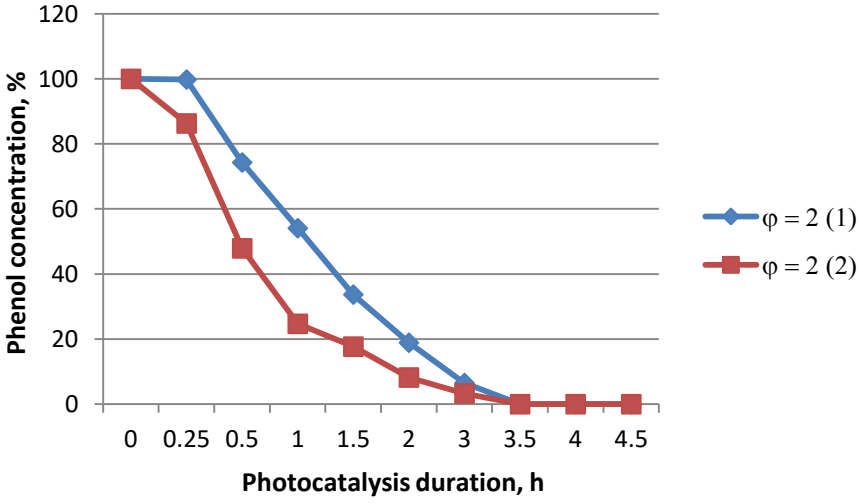

c

Fig. 17. *Change in time under the action of ultraviolet irradiation of the phenol relative concentration in an aqueous solution with a suspension of particles of calcined products of solution combustion (SHS-S) (1) and gel combustion (SHS-G) (2) synthesized at:* ***a*** *– φ=0.25;* ***b*** *– φ=1;* ***c*** *– φ=2*

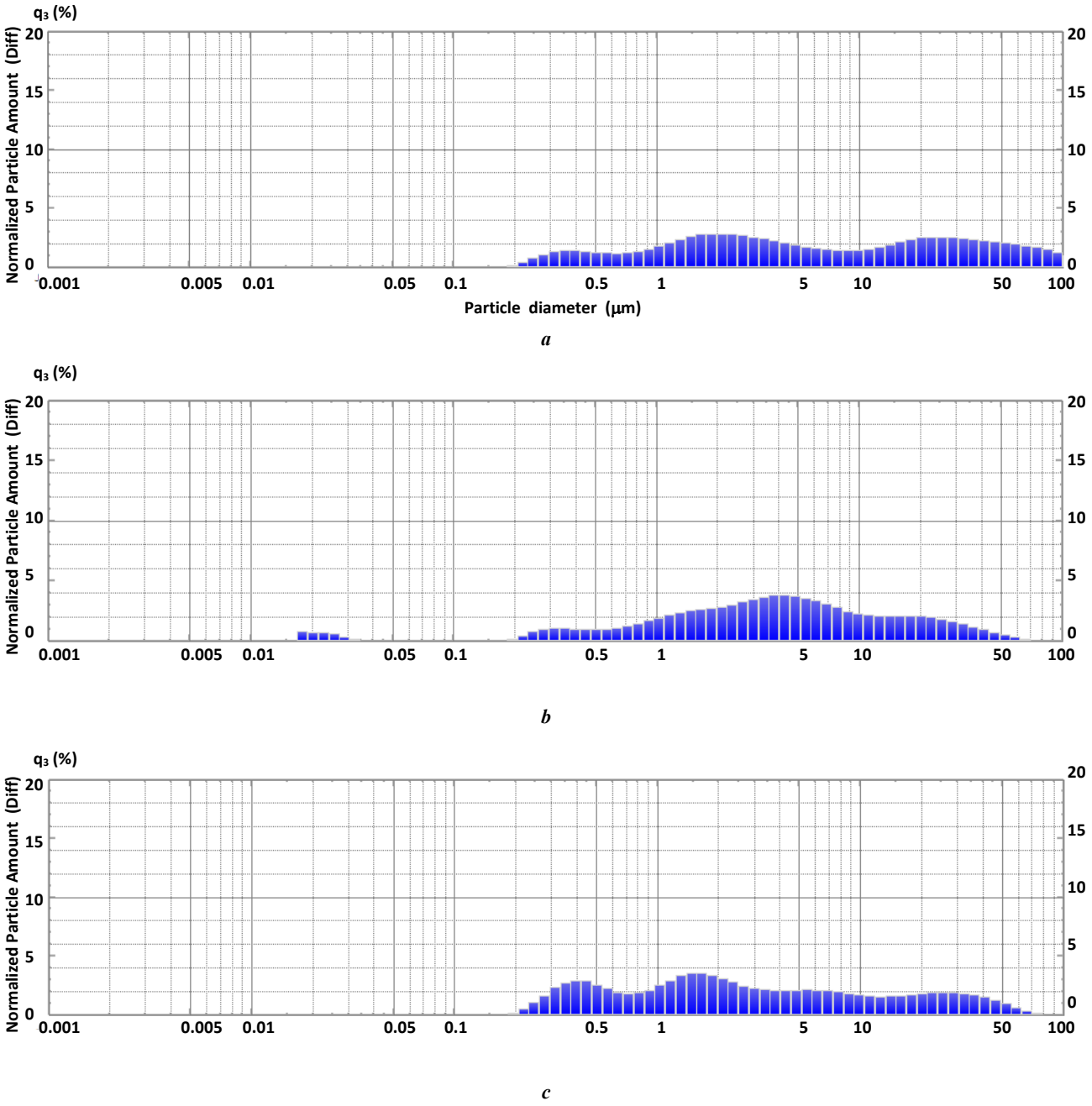

Fig. 18. *The particle-size distribution (the dependence of the normalized particle amount q_3 (%) on the particle diameter) of the calcined and ground in the mortar (10 minutes) SHS-G product synthesized at:* ***a*** *– φ=0.25, D_{50}=5.4 μm;* ***b*** *– φ=1, D_{50}=3.81 μm;* ***c*** *– φ=2, D_{50}=2.37 μm*

the smallest sizes of ZnO particles (Fig. 18). The most active SHS-G product at φ=2 has the smallest average particle size D_{50}=2.37 μm and 90 % of the particles are smaller than 27 μm. In the SHS-G product at φ=1 with an average particle size D_{50}=3.81 μm, even the presence of 4 % of nanoparticles with a size of less than 0.035 μm is observed, and 90 % of the particles have a size of less than 22 μm. The largest particles are at φ=0.25: the average size D_{50}=5.4 μm, 90 % of particles are smaller than 55 μm. However, in some time after the start of ultraviolet irradiation, the photocatalytic activity of the SHS-G and SHS-S products becomes the same, for example, after 3.5 h at φ=2.

DISCUSSION

To increase the photocatalytic activity of zinc oxide synthesized by the solution SHS method, the authors carried out a detailed study of grinding the SHS-S product in a drum ball mill, a planetary centrifugal mill, and a mortar. Intensive grinding in a DBM and PCM leads to a strong sticking of the ground material on the grinding agents and the walls of the mill drums (Fig. 3), which creates great inconvenience due to the necessity of cleaning them; to the darkening of the ground product due to high contamination with iron oxide (30 % after grinding in the DBM and 36 % after grinding in the PCM according to Fig. 5) due to the milling of iron from steel grinding agents and drums; to

the formation of large dense agglomerates from the initial small nanosized and submicron ZnO particles of the synthesized product (Fig. 4). The purest (without iron impurity) and finest ZnO powder is produced by simply grinding the synthesis product in a ceramic mortar.

Non-calcined ZnO powders ground by any method exhibit weak photocatalytic properties during the phenol decomposition (Fig. 9) due to their contamination with up to 10 % carbon (Fig. 5, Table 1). An increase in the phenol concentration by 20 % over 100 % observed in Fig. 9 can be explained by the release of unburned organic fuel residues from porous agglomerates of non-calcined ZnO particles into the solution. These residues have fluorescent properties similar to phenol, and the total concentration of these residues and phenol is reflected in the graph and can exceed 100 % [11]. (Calcination at 650 °C for 1 h and more leads to a significant decrease in the unburned organic fuel residues in the porous agglomerates of ZnO particles. The exceeding of 100 % of the relative phenol concentration in the experiments on the photocatalytic phenol decomposition under the action of ultraviolet irradiation is not observed [11].)

Calcination (oxidative annealing) at 650 °C for 1 h significantly reduces the carbon impurity content in the SHS-S product to a level of 1–2 %, but does not free the product ground in a DBM and PCM from the iron impurity (Fig. 8). The amorphous component from the unburned fuel residues is absent in the structure of calcined products (Fig. 6). The most homogeneous and fine powder structure is obtained after grinding in a mortar (Fig. 7). As a result, the highest photocatalytic activity in the reaction of phenol decomposition in an aqueous solution under the action of ultraviolet irradiation is observed in the calcined ZnO powder ground in a ceramic mortar (Fig. 10). However, this photocatalytic activity does not exceed the photocatalytic activity of the calcined ZnO powder without any grinding given in the work [11].

In such manner, through grinding the nanostructured product of the solution SHS, it was not possible to increase its photocatalytic activity in the phenol decomposition. Firstly, grinding in a ceramic mortar slightly reduces the photocatalytic activity due to an increase in the size of agglomerates of nano- and submicron particles of the ZnO powder. Secondly, grinding in drum ball and planetary centrifugal mills even significantly impairs the photocatalytic activity both due to a greater increase in the size and density of agglomerates of the ZnO powder particle and due to contamination with iron impurities from steel grinding agents and mill drums.

The study of another SHS process variant, when synthesizing ZnO nanopowder from a gel formed from moistened initial dry mixtures of zinc nitrate and glycine (SHS-G process), showed that its characteristics and product, although similar (as can be seen from the comparison of Fig. 1 and Fig. 11, as well as from the description of the products), in some positions they compare favorably with the solution SHS process (SHS-S). Firstly, the SHS-G process is easier and faster to implement, since there is no need to prepare saturated solutions of re-agents, combustion begins much faster (1.5 min on average) than in the case of dissolved re-agents (8 min on average), since in the case of the SHS-S process, a lot of time is spent for heating the solution to boiling water and evaporating water before gel formation. Secondly, the synthesized SHS-G product is finer and cleaner in terms of the content of carbon impurities (Fig. 11–14). The average carbon content in the non-calcined SHS-G product is 1–2 % for different φ criterion values, while in the non-calcined SHS-S product the average carbon content is about 10 % [11]. Calcination at a temperature of 650 °C for 1 h significantly reduces the average content of carbon impurity in the SHS-G product from 2 % for the non-calcined product to 1 % (Fig. 15). On average, about 1 % of carbon is also contained in the SHS-S product after calcinations at 650 °C [11].

Non-calcined SHS-G and SHS-S products have a low photocatalytic activity in the phenol decomposition (Fig. 16), which is slightly higher for the SHS-G product due to the higher purity in terms of the carbon impurity content. The calcinations of the synthesized SHS-G and SHS-S products significantly increases their photocatalytic activity (Fig. 17), especially of the SHS-G products, which contribute to the almost complete phenol decomposition within 3.5–4.5 h of ultraviolet irradiation. Such activity of the products is explained both by their significant purification from carbon impurities during calcinations to a level of 1 % ([11] and Fig. 15) and by the smallest sizes of ZnO particles (Fig. 18). However, the difference between the photocatalytic activity of the SHS-G and SHS-S products, both non-calcined (Fig. 16) and calcined (Fig. 17), in the phenol decomposition, is noticeable only within the first few hours (3.5–5 h in most cases) of ultraviolet irradiation. Then this difference disappears, i.e., the SHS-G and SHS-S products have almost the same photocatalytic activity in the phenol decomposition under the action of ultraviolet irradiation.

Such a result can be explained by the fact that both related processes – the combustion of a solution of an exothermic mixture of initial re-agents of zinc nitrate oxidizer and glycine organic fuel (SHS-S) and the combustion of a gel from a moistened mixture of dry initial re-agents (SHS-G) – lead to the synthesis of almost one and the same product: highly dispersed crystalline powder of zinc oxide ZnO with an admixture of amorphous unburned organic fuel residues in the form of free and combined carbon (Fig. 2 and 13). After the combustion product is calcined in a muffle furnace with an air atmosphere during 1 h at 650 °C, the carbon content decreases to 1 % in average and the calcined synthesis product acquires a uniform powder body structure from the porous agglomerates up to 100 μm in size, sintered from crystalline nanosized and submicron ZnO particles with an average crystallite size of 10 to 50 nm. Such nanostructured zinc oxide demonstrates high photocatalytic activity in the phenol decomposition in an aqueous solution with a suspension of ZnO particles under the action of ultraviolet irradiation leading to almost complete phenol decomposition in less than 4.5 h. This photocatalytic activity is comparable to the activity in the phenol photocatalytic decomposition of ZnO powders with a nanosized substructure obtained by the hydrothermal method after annealing at 650 °C for 3–5 h [14]. At the same time, the SHS-S and SHS-G methods are much more productive than the hydrothermal method, and the synthesized photocatalyst particles are much larger.

The positive aspects of these SHS methods should also include the presence of carbon impurities in their products (up to 1 % in calcined products), which can increase

the photocatalytic activity of synthesized ZnO, as shown in the works [15–17]. Moreover, SHS processes are characterized by an increased defectiveness of synthesized powders due to very high rates of heating and cooling of combustion products, which can also increase their photocatalytic activity [18; 19]. One more advantage of the synthesized ZnO powders is that sufficiently large sintered porous agglomerates up to 100 μm in size from the high-dispersed ZnO particles, with their high photocatalytic activity, can significantly simplify the possibility of their application in the suspension state in a membrane photocatalytic plant for fine water purification. In this case, the separation of the photocatalyst after water purification can be carried out by simple filtration instead of a much more complex and inefficient separation through a ceramic ultrafiltration membrane with a pore size of 100 nm [14].

Consequently, the authors failed to increase the photocatalytic activity in the phenol decomposition of a fine zinc oxide ZnO powder obtained by burning a solution of the zinc nitrate and glycine mixture (the solution SHS method) either by grinding a product of the solution combustion of an exothermic mixture of initial zinc nitrate and glycine re-agents, or by using a combustion product of a gel from a moistened mixture of dry re-agents. The authors of this paper continue to study the possibility of increasing the photocatalytic activity of this powder by doping it with various metal elements (Fe, Mg, Ni, Co), since it is known that such doping can significantly increase the photocatalytic activity of zinc oxide and make it effective in the decomposition of organic water pollutants when irradiated both with visible light and with ultraviolet radiation, which is very important for the practical application of a photocatalyst for the industrial wastewater treatment [20; 21]. Therefore, a simple energy-efficient method of burning mixtures of zinc nitrate with glycine will allow obtaining an inexpensive nanostructured catalyst based on doped zinc oxide with high photocatalytic activity in the phenol decomposition under the action of visible light.

CONCLUSIONS

1. Nanostructured zinc oxide ZnO produced by the method of the solution self-propagating high-temperature synthesis through the combustion of a solution of a mixture of zinc nitrate re-agents, with glycine and subsequent calcination in an oxidizing air atmosphere, has a high photocatalytic activity in the phenol decomposition in an aqueous solution under the action of ultraviolet irradiation, but is ineffective when irradiated with visible light.

2. Grinding of this SHS-S product in a drum ball mill, planetary centrifugal mill, and in a mortar to increase its photocatalytic activity did not lead to a desired result. Intensive grinding in a DBM and PCM is accompanied by a large contamination of the product with iron oxide due to the milling of iron from steel grinding agents and drums, as well as by the formation of large dense agglomerates from the initial small nanosized and submicron ZnO particles, which significantly reduces the photocatalytic activity of the ground product. The purest (without iron impurity) and fine ZnO powder is produced by simply grinding the synthesis product in a ceramic mortar, but its photocatalytic activity does not increase from this.

3. The study of another version of the SHS process, when synthesizing ZnO from a gel formed from the moistened initial dry mixtures of zinc nitrate and glycine (SHS-G process), showed that its characteristics and product, although similar, differ from the SHS-S process. Firstly, it is implemented easier and faster. Secondly, the SHS-G product is smaller and cleaner in terms of the content of carbon impurities. However, the difference between the photocatalytic activity of the SHS-G and SHS-S products in the phenol decomposition is noticeable only at the initial stage of ultraviolet irradiation, after which this difference disappears. The calcined SHS-G and SHS-S products have practically the same high photocatalytic activity in the phenol decomposition under the action of ultraviolet irradiation causing almost complete phenol decomposition in 3.5–4.5 h of ultraviolet irradiation.

4. Neither by grinding the SHS-S product, nor by using the SHS-G method, it was possible to increase the photocatalytic activity in the phenol decomposition of the highly dispersed zinc oxide powder produced by these SHS methods. Probably, the continuation of these studies concerning the use of doping of zinc oxide synthesized by the combustion of mixtures of re-agents with various metal elements (Fe, Mg, Ni, Co) will help to significantly increase its photocatalytic activity and make it effective in the phenol decomposition upon irradiation with visible light.

REFERENCES

1. Anku W.W., Mamo M.A., Govender P.P. Phenolic compounds in water: sources, reactivity, toxicity and treatment methods. *Phenolic Compounds – Natural Sources, Importance and Applications*. Croatia, InTechOpen Publ., 2017, pp. 419–443. DOI: 10.5772/66927.
2. Alberti S., Basciu I., Vocciante M., Ferretti M. Experimental and physico-chemical comparison of ZnO nanoparticles' activity for photocatalytic applications in wastewater treatment. *Catalysts*, 2021, vol. 11, no. 6, pp. 678–691. DOI: 10.3390/catal11060678.
3. Ong C.B., Ng L.Y., Mohammad A.W. A review of ZnO nanoparticles as solar photocatalysts: Synthesis, mechanisms and applications. *Renewable and Sustainable Energy Reviews*, 2018, vol. 81, part 1, pp. 536–551. DOI: 10.1016/j.rser.2017.08.020.
4. Kumar N., Yadav S., Mittal A., Kumari K. Photocatalysis by zinc oxide-based nanomaterials. *Nanostructured Zinc Oxide. Synthesis, Properties and Applications*. The Netherlands, Elsevier Publ., 2021, pp. 393–457. DOI: 10.1016/B978-0-12-818900-9.00005-X.
5. Patil K.C., Hedge M.S., Rattan T., Aruna S.T. *Chemistry of nanocrystalline oxide materials: combustion synthesis, properties and applications*. New Jersey, World Scientific Publ., 2008. 362 p. DOI: 10.1142/6754.
6. González-Cortés L.S., Imbert F.E. Fundamentals, properties and applications of solid catalysts prepared by solution combustion synthesis (SCS). *Applied Catalysis A: General*, 2013, vol. 452, pp. 117–131. DOI: 10.1016/J.APCATA.2012.11.024.
7. Varma A., Mukasyan A.S., Rogachev A.S., Manukyan K.V. Solution combustion synthesis of nanoscale

materials. *Chemical Reviews*, 2016, vol. 116, no. 23, pp. 14493–14586. DOI: 10.1021/acs.chemrev.6b00279.
8. Hwang C.-C., Wu T.-Yu. Synthesis and characterization of nanocrystalline ZnO powders by a novel combustion synthesis method. *Materials Science and Engineering B*, 2004, vol. 111, no. 2-3, pp. 197–206. DOI: 10.1016/j.mseb.2004.04.021.
9. Riahi-Noori N., Sarraf-Mamoory R., Alizadeh P., Mehdikhani A. Synthesis of ZnO nano powder by a gel combustion method. *Journal of Ceramic Processing Research*, 2008, vol. 9, no. 3, pp. 246–249.
10. Zak A.K., Abrishami M.E., Majid W.H.A., Yousefi R., Hosseini S.M. Effects of annealing temperature on some structural and optical properties of ZnO nanoparticles prepared by a modified sol–gel combustion method. *Ceramics International*, 2011, vol. 37, no. 1, pp. 393–398. DOI: 10.1016/j.ceramint.2010.08.017.
11. Amosov A.P., Novikov V.A., Kachkin E.M., Kryukov N.A., Titov A.A., Sosnin I.M., Merson D.L. The solution combustion synthesis of ZnO powder for the photodegradation of phenol. *Ceramics*, 2022, vol. 5, no. 4, pp. 928–946. DOI: 10.3390/ceramics5040067.
12. Khaliullin S.M., Zhuravlev V.D., Ermakova L.V., Buldakova L.Y., Yanchenko M.Y., Porotnikova N.M. Solution combustion synthesis of ZnO using binary fuel (glycine + citric acid). *International Journal of Self-Propagating High-Temperature Synthesis*, 2019, vol. 28, no. 4, pp. 226–232. DOI: 10.3103/S1061386219040058.
13. Ermakova L.V., Zhuravlev V.D., Khaliullin Sh.M., Vovkotrub E.G. Thermal analysis of the products of SCS of zinc nitrate with glycine and citric acid. *Thermochimica Acta*, 2020, vol. 695, article number 178809. DOI: 10.1016/j.tca.2020.178809.
14. Vikarchuk A.A., Sosnin I.M., Stepanov S.V., Stepanov A.S. Nanotechnology for deep sewage treatment of airports from toxic pollution, materials and equipment for its implementation. *Vodoochistka. Vodopodgotovka. Vodosnabzhenie*, 2018, no. 12, pp. 18–23. EDN: YPXEFV.
15. Haibo O., Feng H.J.F., Cuiyan Li., Liyun C., Jie F. Synthesis of carbon doped ZnO with a porous structure and its solar-light photocatalytic properties. *Materials Letters*, 2013, vol. 111, pp. 217–220. DOI: 10.1016/j.matlet.2013.08.081.
16. Bechambi O., Sayadi S., Najjar W. Photocatalytic degradation of bisphenol A in the presence of C-doped ZnO: effect of operational parameters and photodegradation mechanism. *Journal of Industrial and Engineering Chemistry*, 2015, vol. 32, pp. 201–210. DOI: 10.1016/j.jiec.2015.08.017.
17. Pan L., Muhammad T., Ma L., Huang Z.-F., Wang S., Wang L., Zou J.-J., Zhang X. MOF-derived C-doped ZnO prepared via a two-step calcination for efficient photocatalysis. *Applied Catalysis B: Environmental*, 2016, vol. 189, pp. 181–191. DOI: 10.1016/j.apcatb.2016.02.066.
18. Xanthopoulou G. Catalytic properties of the SHS products. Review. *Advances in Science and Technology*, 2010, vol. 63, pp. 287–296. DOI: 10.4028/www.scientific.net/AST.63.287.
19. Al-Sabahi J., Bora T., Al-Abri M., Dutta J. Controlled defects of zinc oxide nanorods for efficient visible light photocatalytic degradation of phenol. *Materials*, 2016, vol. 9, no. 4, article number 238. DOI: 10.3390/ma9040238.
20. Reddy I.N., Reddy C.V., Shim J., Akkinepally B., Cho M., Yoo K., Kim D. Excellent visible-light driven photocatalyst of (Al, Ni) co-doped ZnO structures for organic dye degradation. *Catalysis Today*, 2020, vol. 340, pp. 277–285. DOI: 10.1016/j.cattod.2018.07.030.
21. Nadeem M.S., Munawar T., Mukhtar F., Rahman M.N., Riaz M., Iqbal F. Enhancement in the photocatalytic and antimicrobial properties of ZnO nanoparticles by structural variations and energy bandgap tuning through Fe and Co co-doping. *Ceramics International*, 2021, vol. 47, no. 8, pp. 11109–11121. DOI: 10.1016/j.ceramint.2020.12.234.